

## Phugoid oscillations in optimal reentry trajectories†

N. X. VINH, J. S. CHERN‡ AND C. F. LIN

The University of Michigan, Ann Arbor, MI 48109, U.S.A.

(Received 7 October 1980)

**Abstract**—A major problem with operations of lifting reentry vehicle having an aft center-of-gravity location due to large engine mass at the rear is the required hypersonic trim to flight the desired trajectory. This condition is most severe for lifting maneuvers. As a first step toward analyzing this problem, this paper considers the lift requirement for some basic maneuvers in the plane of a great circle. Considerations are given to optimal lift control for achieving the maximization of either the final altitude, speed or range. For the maximum-range problem, phugoid oscillation along an optimal trajectory is less severe as compared to a glide with maximum lift-to-drag ratio. An explicit formula for the number of oscillations for an entry from orbital speed is proposed.

### Introduction

IN THIS last part of the century, space activities will be centered around the operations of the space shuttle, a versatile hypervelocity vehicle capable of reentering the Earth's atmosphere and using its lifting characteristics for aerodynamic maneuvering. The following generation of advanced earth orbital transportation systems are currently being studied by NASA to assess their potential cost/performance payoff. The baseline system chosen to investigate is a fully reusable single-stage-to-orbit vehicle capable of vertical take-off and horizontal landing. For this type of vehicle, an aft center-of-gravity location resulting from large engine mass at the rear of the vehicle has been a continuing problem in terms of dynamic stability and control (Freeman and Powell, 1979).

In longitudinal dynamics, the two main modes of oscillations are the phugoid mode and the angle-of-attack mode. Phugoid oscillation is basically a trajectory oscillation along which the center of mass of the vehicle oscillates about a reference trajectory through an exchange between the kinetic energy and the potential energy of the system. The oscillation is particularly pronounced for a glide entry. Although, for at least through the next decade, reentry vehicles are designed for near ballistic entry through the hypersonic regime (Stone and Powell, 1977; Freeman and Wilhite, 1979), it is of interest to investigate some of their basic lifting maneuvers since these will require the most severe conditions on hypersonic trim to flight the desired trajectory.

For this investigation, Chapman's variables (Chapman, 1959) have been used to put the equations in dimensionless form applicable to any arbitrary configuration of the reentry vehicle. Particular considerations are given to optimal

---

†Work supported by NASA Grant No. NAG 1-86

‡Chung Shan Institute of Science and Technology, Taiwan, R.O.C.

maneuvers for achieving the maximization of a certain performance index to be specified.

### The variational equations

Using standard notation with the nomenclature depicted in Fig. 1, the motion of a non-thrusting, lifting vehicle entering a stationary and spherical planetary atmosphere is governed by the equations:

$$\begin{aligned}\frac{dr}{dt} &= V \sin \gamma, \\ \frac{dV}{dt} &= -\frac{\rho S C_D V^2}{2m} - g \sin \gamma, \\ V \frac{d\gamma}{dt} &= \frac{\rho S C_L V^2}{2m} - \left(g - \frac{V^2}{r}\right) \cos \gamma, \\ \frac{d\theta}{dt} &= \frac{V \cos \gamma}{r}.\end{aligned}\quad (1)$$

We shall use a parabolic drag polar

$$C_D = C_{D_0} + K C_L^2 \quad (2)$$

and a normalized lift coefficient

$$\lambda = C_L / \sqrt{C_{D_0} / K} \quad (3)$$

for the lift control. In this way  $\lambda = 1$  corresponds to maximum lift-to-drag ratio  $E^*$  with

$$E^* = \frac{1}{2\sqrt{K C_{D_0}}}. \quad (4)$$

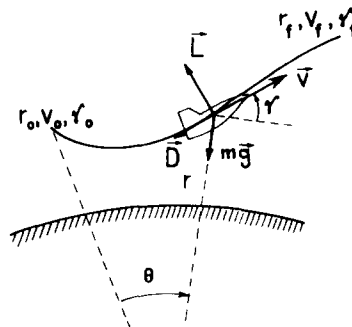


Fig. 1. Nomenclature.

With a locally exponential atmosphere, a Newtonian gravitational attraction, and the use of the modified Chapman's variables

$$Z = \frac{\rho S}{2m} \sqrt{\left(\frac{rC_{D0}}{\beta K}\right)}, \quad v = \frac{V^2}{gr} \quad (5)$$

for the altitude and speed variable, respectively, the following dimensionless equations are deduced (Vinh *et al.*, 1975):

$$\begin{aligned} \frac{dZ}{d\theta} &= -k^2 Z \tan \gamma, \\ \frac{dv}{d\theta} &= -\frac{kZv(1+\lambda^2)}{E^* \cos \gamma} - (2-v) \tan \gamma, \\ \frac{d\gamma}{d\theta} &= \frac{kZ\lambda}{\cos \gamma} + \left(1 - \frac{1}{v}\right), \\ \frac{d\theta}{d\theta} &= 1. \end{aligned} \quad (6)$$

In this formulation, the characteristic of the vehicle is represented by the maximum lift-to-drag ratio,  $E^*$ , while the property of the atmosphere is specified by the constant  $k^2 = \beta r$ . For the numerical computation, we shall take  $E^* = 3$  and  $k^2 = 900$  as a representative value for the Earth's atmosphere. The last equation in system (6) is introduced to retain the range angle as state variable. The single control is the normalized lift coefficient  $\lambda$  subject to the constraint:

$$|\lambda| \leq \lambda_{\max}. \quad (7)$$

Using the maximum principle, we introduce the adjoint vector  $\mathbf{p}$  to form the Hamiltonian:

$$\begin{aligned} H &= p_\theta - k^2 Z p_Z \tan \gamma - p_v \left[ \frac{kZv(1+\lambda^2)}{E^* \cos \gamma} + (2-v) \tan \gamma \right] \\ &+ p_\gamma \left[ \frac{kZ\lambda}{\cos \gamma} + \left(1 - \frac{1}{v}\right) \right]. \end{aligned} \quad (8)$$

The two integrals of the variational problem are

$$p_\theta = C, \quad H = 0. \quad (9)$$

Hence, only two of the three remaining adjoint variables are to be found. For the most general free-time problem, through normalizing of the adjoints we only need to estimate two arbitrary constants for obtaining the optimal solution to the

problem considered. In particular, for a free-range problem,  $C = 0$ , the problem is reduced to a one-parameter problem. To show this, we first deduce that the optimal lift control is either on the boundary,  $|\lambda| = \lambda_{\max}$ , or in the interior, with a modulated lift coefficient such that

$$\lambda = \frac{E^* p_\gamma}{2v p_v}. \quad (10)$$

For this control, the adjoint equations are:

$$\begin{aligned} \frac{dp_Z}{d\theta} &= k^2 p_Z \tan \gamma + p_v \frac{kv(1+\lambda^2)}{E^* \cos \gamma} - p_\gamma \frac{k\lambda}{\cos \gamma}, \\ \frac{dp_v}{d\theta} &= p_v \left[ \frac{kZ(1+\lambda^2)}{E^* \cos \gamma} - \tan \gamma \right] - \frac{p_\gamma}{v^2}, \\ \frac{dp_\gamma}{d\theta} &= \frac{1}{\cos^2 \gamma} \left\{ k^2 Z p_Z + p_v \left[ \frac{kZv(1+\lambda^2) \sin \gamma}{E^*} + (2-v) \right] \right. \\ &\quad \left. - kp_\gamma Z \lambda \sin \gamma \right\}. \end{aligned} \quad (11)$$

By taking the derivative of eqn (10), using the state and adjoint equations, we have the equation for the modulated lift control:

$$\frac{d\lambda}{d\theta} = \frac{kZ(1-\lambda^2) \sin \gamma}{2 \cos^2 \gamma} + \frac{2\lambda(\lambda + E^* \tan \gamma)}{E^* v} + \frac{E^*}{2 \cos^2 \gamma} \left( F - 1 + \frac{2}{v} \right), \quad (12)$$

where  $F$  is the ratio

$$F = \frac{k^2 Z p_Z}{v p_v}. \quad (13)$$

By taking the derivative of this equation, we have the equation for  $F$ :

$$\frac{dF}{d\theta} = \frac{k^3 Z(1-\lambda^2)}{E^* \cos \gamma} + \frac{2F}{E^* v} (\lambda + E^* \tan \gamma). \quad (14)$$

The Hamiltonian integral becomes

$$\frac{kZ(1-\lambda^2)}{E^* \cos \gamma} + \frac{2(1-v)\lambda}{E^* v} + \left( F - 1 + \frac{2}{v} \right) \tan \gamma = \frac{C}{v p_v}. \quad (15)$$

The variational system consists of the three state equations, eqns (6) for  $Z$ ,  $v$  and  $\gamma$ , eqn (12) for the optimal lift control  $\lambda$ , and eqn (14) for the additional adjoint  $F$ . Since the initial values of the state variables are prescribed, the

integration of the system requires selecting two arbitrary initial values  $\lambda_0$  and  $F_0$  for  $\lambda$  and  $F$ . These values are to be found such that the final and transversality conditions are identically satisfied. In particular, if the final flight path angle is free,  $p_\gamma(\theta_f) = 0$ , and hence

$$\lambda_f = 0. \quad (16)$$

In the case where the range is free,  $C = 0$ . The Hamiltonian integral, eqn (15), evaluated at the initial time, provides  $\lambda_0$  in terms of  $F_0$  or vice versa. The problem is a one-parameter problem.

As applications, we shall consider the following problems.

### Optimal pull-up maneuver

The range is free, and hence the only arbitrary parameter involved is the initial lift coefficient  $\lambda_0$ . The initial condition is

$$\theta = 0, \quad Z = Z_0, \quad v = v_0, \quad \gamma = \gamma_0. \quad (17)$$

It is proposed to find the optimal lift control to bring the vehicle from this initial condition to the final instant,  $\theta_f = \text{free}$ , such that either

$$Z = Z_f, \quad v_f = \text{max.}, \quad (18)$$

or

$$v = v_f, \quad Z_f = \text{min.} \quad (19)$$

The first condition is the condition of maximum final speed when the vehicle reaches a prescribed final altitude. The second condition is the condition of maximum final altitude for a prescribed final speed. The two problems are equivalent and they are solved by a single routine. For the numerical computation, we take  $Z = 0.5$ ,  $v_0 = 0.15$ ,  $\gamma_0 = -1/2 E^*$ , with  $E^* = 3$  and  $k^2 = 900$  for the Earth's atmosphere. Since  $\gamma_f$  is free, for a totality of the family of optimal trajectories, it suffices to use  $\lambda_0$  as parameter for integration until  $\lambda_f = 0$ . The solution is given in Fig. 2 as the plot of the altitude gain, or loss, versus the speed ratio  $V/V_0$ . Through the use of the dimensionless variables, we deduce the variation in the altitude:

$$\beta \Delta h = \beta(h - h_0) = \log \left( \frac{Z_0}{Z} \right), \quad (20)$$

which is independent of the physical characteristics of the vehicle. In the figure, the solid lines are the different optimal trajectories leading to the terminal boundary in dashed line. Along this boundary we can read the maximum altitude gain for any prescribed loss in the speed, or the resulting maximized final speed for any prescribed final altitude. Low initial values of the lift coefficient

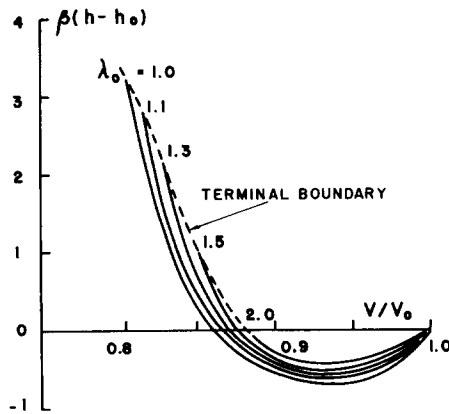


Fig. 2. Solution for the optimal pull-up maneuver.

correspond to high final altitudes. The variation of the optimal lift coefficient is shown in Fig. 3. For low final altitudes,  $\lambda$  decreases from the initial value to zero at the final time while for high final altitude, the lift coefficient first increases slowly to a maximum value and then decreases to zero. The lift coefficients for different trajectories pass through nearly the same value just after passage through the lowest point,  $\gamma = 0$ . For all these pull-up trajectories, the flight path angle increases from the initial negative value, passes through a maximum during the ascending phase and then decreases. At that point, the trajectory has an inflection point.

**Skip trajectory for maximum range**

In a skip trajectory, the vehicle enters the atmosphere at very high altitude at a speed at orbital magnitude and uses its lifting capability to negotiate a turn in the vertical plane. It is then ejected from the atmosphere and the following arc

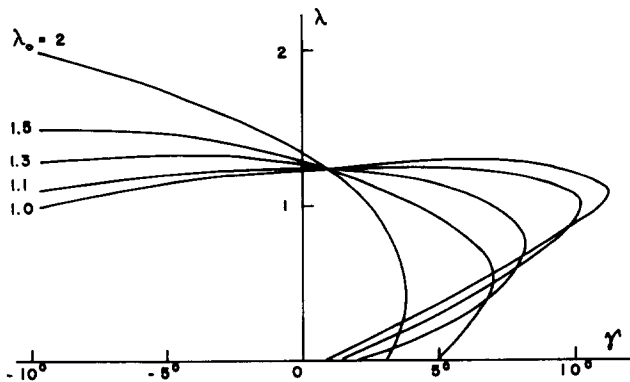


Fig. 3. Variation of the optimal lift coefficient for pull-up maneuver.

becomes Keplerian. This maneuver is depicted in Fig. 4. The skip maneuver is an important maneuver. It can be used to achieve maximum range. This is because if the initial speed is sufficiently high, the Keplerian arc following each skip can contribute significantly to the total range, while a trajectory totally immersed inside the atmosphere is destined to have limited range.

For a vehicle entering the atmosphere, we must start the integration with some non-zero initial value  $Z_0$  of  $Z$ . We shall adopt the convention that atmospheric entry is initiated when the acceleration due to atmospheric lift is equal to a certain small fraction of the gravity acceleration. From the definition (5) of  $Z$  and  $v$ , the dimensionless acceleration due to lift force at maximum lift-to-drag ratio is:

$$\frac{a}{g} = kZv. \quad (21)$$

Taking  $a/g = 0.015$ , with an initial speed equal to orbital speed,  $v_0 = 1.0$ , we have the value  $Z_0 = 0.0005$ . After the skip, beyond the exit point  $Z_f = Z_0$ , the flight is considered purely Keplerian providing the coasting range  $2\xi$  until the next atmospheric phase. The problem of maximum range is first solved by considering the value  $\theta_f$  at the exit point as free, and hence  $C = 0$ . This is suggested by the fact that at orbital speed with small value of  $\gamma_0$ , the coasting range  $2\xi$  is significantly larger and more sensitive to change than the atmospheric skip range  $(\theta_f - \theta_0)$ . The next case to be addressed is the maximization of the total range  $(\theta_f - \theta_0) + 2\xi$ .

From Keplerian motion, it can be shown that the performance index to be maximized is

$$J = \frac{1}{\cos \xi} = \frac{\sqrt{(1 - v_f(2 - v_f) \cos^2 \gamma_f)}}{1 - v_f \cos^2 \gamma_f}, \quad (22)$$

where subscript  $f$  denotes the condition at exit point. Since  $\theta_f$  is free, the sole

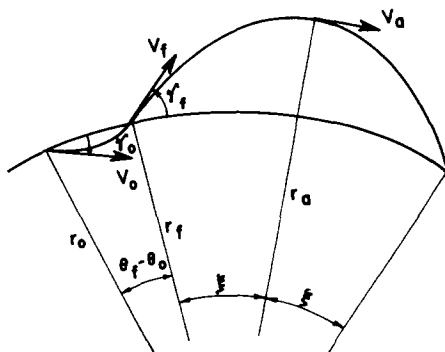


Fig. 4. Geometry of a skip trajectory.

parameter is  $\lambda_0$ . It is to be selected for the integration such that at the final time, the transversality condition

$$p_{v_f} = \frac{\partial J}{\partial v_f}, \quad p_{\gamma_f} = \frac{\partial J}{\partial \gamma_f} \quad (23)$$

is satisfied. From eqn (10), this leads to the condition:

$$\lambda_f = \frac{E^*(1 - v_f - \tan^2 \gamma_f)}{2 \tan \gamma_f}, \quad (24)$$

which must be satisfied by  $\lambda$  at the final time. As numerical example, we have the following optimal trajectory:

$$\begin{aligned} Z_0 &= 0.0005, & v_0 &= 1.0, & \gamma_0 &= -4^\circ \\ Z_f &= 0.0005, & v_f &= 0.87475, & \gamma_f &= 6.02^\circ \\ \lambda_0 &= 0.2925, & \theta_f - \theta_0 &= 0.17646, & 2\xi_{\max} &= 1.18958 \end{aligned}$$

To show the optimality character of this trajectory, we integrate the state equations (6), using a constant lift coefficient,  $\lambda = \text{constant}$ . The best constant  $\lambda$  which gives the maximum coasting range is found to be  $\lambda = 1.024$ , and the corresponding results are:

$$\begin{aligned} Z_f &= 0.0005, & v_f &= 0.90876, & \gamma_f &= 3.58^\circ \\ \theta_f - \theta_0 &= 0.20633, & 2\xi_{\max} &= 1.07743. \end{aligned}$$

It shows that, using optimal lift modulation we have an improvement of 10.41% in the coasting range as compared to the best solution obtained with a constant lift coefficient.

We now solve the second case, in which we maximize the total range from the initial point to the end of the coasting flight. The performance index to be maximized is then

$$J = (\theta_f - \theta_0) + 2 \arccos \left[ \frac{1 - v_f \cos^2 \gamma_f}{\sqrt{(1 - v_f)(2 - v_f) \cos^2 \gamma_f}} \right]. \quad (25)$$

This time, the final range is not free, and hence  $C \neq 0$ . There are two parameters,  $\lambda_0$  and  $F_0$ , to be found. In addition to condition (23), we have  $C = p_{\theta_f} = \partial J / \partial \theta_f = 1$ . By comparing the eqns (22) and (25), it is clear that the condition (24) remains enforced in this problem. We need one more transversality condition because this case has two parameters. It comes from the Hamiltonian integral (15) evaluated at the final time. With  $C = 1$  and  $p_{v_f}$  obtained from eqn (23) with  $J$  as given by eqn (25), we have upon using eqn (24) for simplification

$$\frac{kZ_f v_f (1 - \lambda_f^2)}{E^* \cos \gamma_f} + \frac{(1 - v_f) \lambda_f}{E^*} + \left( 1 - \frac{1}{2} v_f + v_f F_f \right) \tan \gamma_f = 0. \quad (26)$$



The transversality conditions (24) and (26), applied at the final time  $Z = Z_f$ , are used to adjust the initial values  $\lambda_0$  and  $F_0$  required for the integration.

The problem is solved and, this time, it is found that

$$\begin{aligned} Z_f &= 0.0005, & v_f &= 0.88101, & \gamma_f &= 5.63^\circ, \\ \lambda_0 &= 0.57921, & F_0 &= 3.6873, \\ \theta_f - \theta_0 &= 0.18173, & 2\xi &= 1.18692. \end{aligned}$$

The total range obtained is  $J = (\theta_f - \theta_0) + 2\xi = 1.36865$ , which is slightly higher than the total range  $J = 1.36604$  of the first case where only the coasting range is maximized.

### Glide trajectory for maximum range

We now use the same initial condition at entry to find the optimal trajectory which maximizes the total range until a final low speed  $v_f = 0.001$  is reached. This speed is of the order of the speed of sound at low altitude. Since the equations derived lead to Keplerian motion when  $Z \rightarrow 0$ , we can integrate them through the near ballistic phase in the vacuum. The initial values  $\lambda_0$  and  $F_0$  are to be selected such that at  $v = v_f$ , for free  $\gamma_f$ ,  $\lambda_f = 0$  and in addition

$$kZ_f v_f = 1. \quad (27)$$

This condition expresses that at the final time the acceleration due to the lift is equal to the gravity acceleration. The variation of the altitude as function of the range for the optimal trajectory is plotted in Fig. 5 as a solid line. The dashed line is the plot of the trajectory with maximum lift-to-drag ratio,  $\lambda = 1$ . The amplitude of oscillation is larger for flight at maximum lift-to-drag ratio. At the beginning, the vehicle skips out repeatedly into the vacuum. For this case, there are two skips along the optimal trajectory and three skips along the trajectory

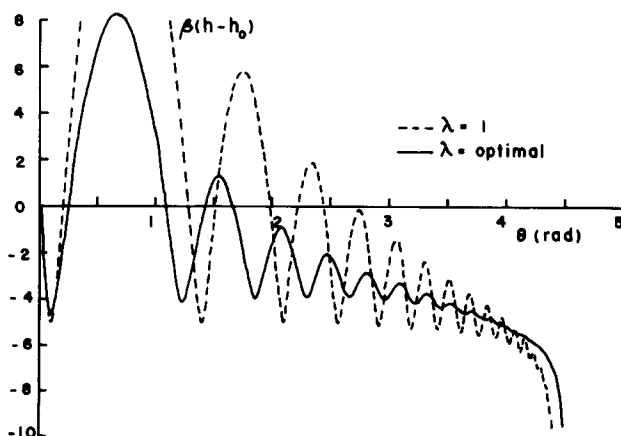


Fig. 5. Variation of the altitude for maximum-range glide.

with maximum lift-to-drag ratio. Hence, besides a range improvement of about 2%, the optimal trajectory with less variation in the altitude is more suitable to an efficient guidance program. The reason that the improvement is relatively small is that the entry condition at orbital speed,  $v_0 = 1.0$ , with small entry angle is ideal for an equilibrium glide at maximum lift-to-drag ratio. With either higher or lower initial speed the difference in the range angle is more pronounced. Figure 6 shows the variation of the flight path angle. While along the optimal trajectory, the flight path angle oscillates near the value zero, the amplitude of oscillation in a maximum lift-to-drag ratio program is larger. Finally, Fig. 7 plots the variation of the optimal normalized lift coefficient and the variation of the speed ratio. It is seen that  $\lambda$  oscillates near the value unity for maximum lift-to-drag ratio and tends to this value at low altitude. This means that, at low speed, the optimal trajectory is practically at maximum lift-to-drag ratio.

With the variational equations available, while it is easy to obtain the solution to any one-parameter problem, for a two-parameter problem and specially for the problem of glide with maximum range requiring a long integration the numerical solution is difficult to obtain using the indirect method through the maximum principle. This is because the trajectory generated is very sensitive to the initial values of the adjoints which are here represented by  $\lambda$  and  $F$ . The values of  $\lambda_0$  and  $F_0$  have to be evaluated with great accuracy to avoid a premature termination of the integration when either  $\lambda$  becomes very large or tending to zero. Fortunately, the equations in  $\lambda$  and  $F$  are fairly stable with a backward integration. This is because at down range  $\lambda$  tends to unity and  $d\lambda/d\theta$  stays near zero. This leads to the following procedure. A trajectory using  $\lambda = 1$  is generated providing a set of values  $Z_1, v_1$  at a certain arbitrary low speed of the order of the speed of sound. The point considered will insure that  $\lambda \approx 1$  and can be taken exactly equal to unity. An average value  $\gamma_1$  can also be evaluated. Starting with  $Z_1, \gamma_1$  and  $\lambda_1 = 1$ , and using  $v_1$  and  $F_1$  as arbitrary parameters, the equations can be integrated backward until  $v_0$ . A good initial value  $F_1$  can be obtained by using  $(d\lambda/d\theta)_1 = 0$ . At  $v = v_0$ , the prescribed condition on  $Z_0$  and  $\gamma_0$  are used for the iteration. Since at the start of the integration a slight variation in

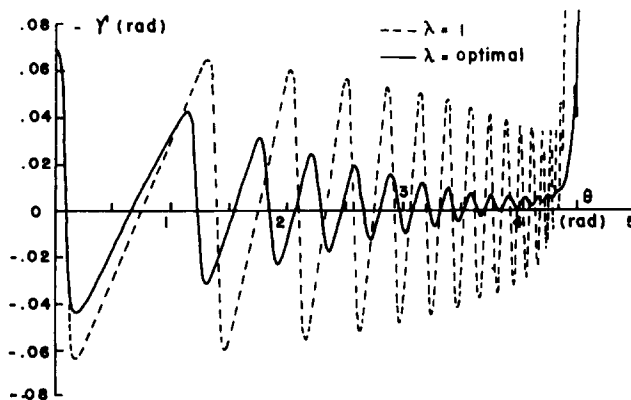


Fig. 6. Variation of the flight path angle for maximum-range glide.

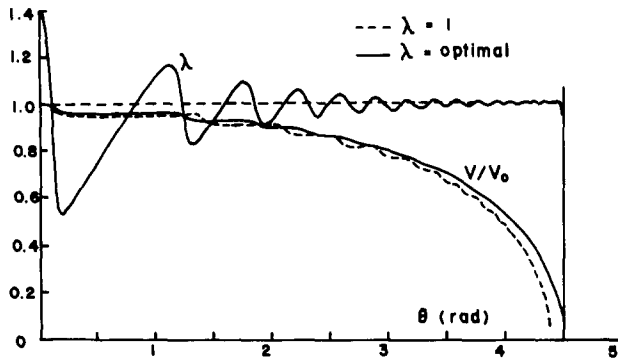


Fig. 7. Variations of the optimal lift coefficient and the speed for maximum-range glide.

$v$  does not significantly change the range and the slope  $d\lambda/d\theta$  is small, the parameters selected for iteration are not sensitive. After a few adjustments, the trajectory leading to the initial point is obtained. A small portion of the range from the speed  $v_1$  to the final prescribed speed  $v_f$  can be added by forward integration. The technique proposed is very efficient and trajectories generated with various values of  $E^*$  from the prescribed initial conditions  $Z_0 = 0.0005$ ,  $v_0 = 1.0$ ,  $\gamma_0 = -4^\circ$  are presented in Figs. 8 and 9.

### Phugoid oscillation

As seen in Fig. 8, a typical characteristic of maximum-range glide is the oscillation in the altitude. This exchange between the potential energy and the kinetic energy is called the phugoid oscillation. From Fig. 5, we notice that the period of oscillation is about the same for both the maximum lift-to-drag ratio glide and the optimal glide. It is larger at high altitude and decreases as the altitude decreases. This is to be expected since when  $Z \rightarrow 0$ , the motion is

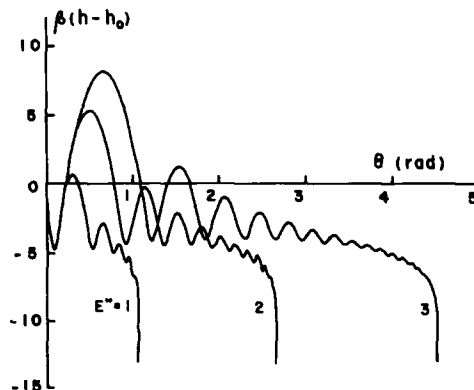


Fig. 8. Variation of the altitude for maximum-range glide for different values of  $E^*$ .

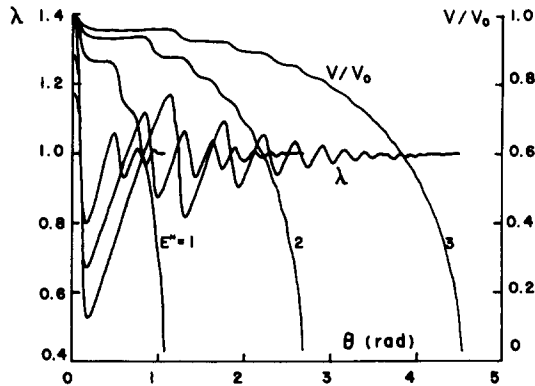


Fig. 9. Variations of the optimal lift coefficient and the speed for maximum-range glide for different values of  $E^*$ .

Keplerian and the period of oscillation is the orbital period while at low altitude, an approximate expression for the phugoid period is  $T = \pi\sqrt{2(2)V/g}$  (Vinh and Dobrzelecki, 1969). Hence, in terms of  $\theta$ , the phugoid period decreases from  $2\pi$  and tends to  $\pi\sqrt{2v}$  at low speed. To find the period of phugoid oscillation, we consider the trajectory with maximum lift-to-drag ratio,  $\lambda = 1$ , and small flight path angle,  $\gamma \approx 0$ . Then the state equations become:

$$\begin{aligned} \frac{dZ}{d\theta} &= -k^2 Z \gamma, \\ \frac{dv}{d\theta} &= -\frac{2kZv}{E^*}, \\ \frac{d\gamma}{d\theta} &= kZ + 1 - \frac{1}{v}. \end{aligned} \tag{28}$$

If the flight path angle varies slowly,  $d\gamma/d\theta \approx 0$ , and we have the so-called equilibrium glide condition

$$kZ = \frac{1-v}{v}. \tag{29}$$

This leads to the change of variable

$$Y = \frac{kZv}{1-v} - 1, \tag{30}$$

where  $Y$  is treated as a small quantity except at the beginning where  $Y$  can be large. Using  $v$  as the independent variable, eqns (28), with the change of variable

(30), become

$$\frac{dY}{dv} = \frac{E^*k^2\gamma}{2(1-v)} + \frac{Y+1}{v(1-v)},$$

$$\frac{d\gamma}{dv} = -\frac{E^*Y}{2v(Y+1)}. \quad (31)$$

By eliminating  $\gamma$  between these two equations, we have a second-order non-linear differential equation for  $Y$

$$v(1-v)\frac{d^2Y}{dv^2} - (1+v)\frac{dY}{dv} + \frac{E^*k^2Y}{4(Y+1)} + \frac{(Y+1)}{v} = 0. \quad (32)$$

The equilibrium solution, eqn (29), does not provide the oscillation in the altitude but gives an average value with good accuracy. Hence, the function  $Y$  gives the oscillation and tends to zero near the end of the trajectory. By linearizing this equation, we obtain:

$$v(1-v)\frac{d^2Y}{dv^2} - (1+v)\frac{dY}{dv} + \left(\frac{E^*k^2}{4} + \frac{1}{v}\right)Y = -\frac{1}{v}. \quad (33)$$

Since the parameter  $E^*k^2/4$  is large, in the homogeneous equation, when  $v$  is not too small, we can neglect the term  $1/v$  and obtain a hypergeometric equation. In general, with the change of variables

$$Y = \frac{U}{(\tan \tau)^{3/2}}, \quad v = \cos^2 \tau, \quad 0 \leq \tau \leq \frac{\pi}{2}, \quad (34)$$

the linear equation (33) is transformed into

$$\frac{d^2U}{d\tau^2} + \left[ E^*k^2 + \frac{1-4\cos^2\tau}{4\sin^2\tau\cos^2\tau} \right]U = -\frac{4\sin\tau(\tan\tau)^{1/2}}{\cos^3\tau}. \quad (35)$$

In the homogeneous equation, the non-constant term in the coefficient of  $U$  is:

$$\frac{1-4\cos^2\tau}{4\sin^2\tau\cos^2\tau} = \frac{1-4v}{4v(1-v)}. \quad (36)$$

In the range of speed of interest, when  $v$  decreases from 0.95 to 0.01, this coefficient increases from a negative value  $-14.737$  to a positive value  $24.242$ . On the other hand, the term  $E^*k^2$  is very large. Hence, the solution of the homogeneous equation in  $Y$  is practically:

$$Y = \frac{1}{(\tan \tau)^{3/2}} [A_1 \cos(E^*k\tau) + A_2 \sin(E^*k\tau)]. \quad (37)$$

To this equation, we add a particular solution of eqn (35). Considering the solution (37), when  $v \rightarrow 0$ ,  $\tan \tau \rightarrow \infty$  and  $Y \rightarrow 0$  as expected. Furthermore,  $Y$ , and hence the "altitude"  $Z$  by eqn (30), has an oscillatory motion in  $\tau$  with frequency  $E^*k$ . Actually, this should be viewed as an oscillation about the mean value given by the equilibrium equation (29) which has been used as the reference solution in the linearization. When  $\tau$  varies from 0 to  $\pi/2$ , the argument of the trigonometric functions in eqn (37) varies from 0 to  $E^*k\pi/2$ . Hence, the number of oscillations is approximately:

$$n = \frac{E^*k}{4}. \quad (38)$$

Finally, it should be noticed that the constant frequency  $E^*k$  is with respect to  $\tau$ . With respect to  $\theta$ , we use the solution for equilibrium glide, eqn (29) to write the equation for  $v$ :

$$\frac{dv}{d\theta} = -\frac{2(1-v)}{E^*}. \quad (39)$$

Integrating and changing to  $\tau$ , we obtain:

$$\frac{\sin \tau}{\sin \tau_0} = e^{\theta/E^*}. \quad (40)$$

Because of the exponential function, when  $\tau$  is plotted versus  $\theta$ , it varies slowly at the beginning and more rapidly for larger  $\theta$ . Hence, with respect to  $\theta$ , the period of oscillation decreases during the glide.

## References

- Chapman D. R. (1959) An approximate analytical method for studying entry into planetary atmosphere. *NASA TR-R-11*.
- Freeman C. D. and Powell R. W. (1979) The results of studies to determine the impact of far-aft center-of-gravity locations on the design of a single-stage-to-orbit vehicle system. *AIAA paper No. 79-0892*, presented at the *AIAA Conf. on Advanced Technology for Future Space Systems*, Hampton, Virginia.
- Freeman C. D. and Wilhite A. W. (1979) Effects of relaxed static longitudinal stability on a single-stage-to-orbit vehicle design. *NASA TP 1594*.
- Stone H. W. and Powell R. W. (1977) Entry dynamics of space shuttle orbiter with longitudinal stability and control uncertainties at supersonic and hypersonic speeds. *NASA TP 1084*.
- Vinh N. X., Busemann A. and Culp R. D. (1975) Optimum three-dimensional atmospheric entry. *Acta Astron.* 2, 593-611.
- Vinh N. X. and Dobrzelecki A. (1969) Non-linear longitudinal dynamics of an orbital lifting vehicle. *NASA CR-1449*.